# Proton Conductivity of Acid-Functionalized Zeolite Beta, MCM-41, and MCM-48: Effect of Acid Strength

John C. McKeen,[†] Yushan S. Yan,[‡] and Mark E. Davis*,[†]

*Chemical Engineering, California Institute of Technology, 1200 East California Boulevard, MC210-41, Pasadena, California 91125, and Department of Chemical and Environmental Engineering, University of California, Riverside, Riverside, California, 92521*

*Received May 25, 2008*
*Revised Manuscript Received July 1, 2008*

Direct methanol fuel cells (DMFCs) and hydrogen proton exchange membrane fuel cells (PEMFCs) are two types of fuel cells where commercial products have been developed, but have yet to find widespread deployment. Although these devices are compact, easily refuelable, and operate at comparatively low temperatures, problems such as catalyst poisoning, methanol crossover, and water management exist and are current topics of research. One important component of both the DMFC and PEMFC is a protonically conducting but electronically insulating membrane placed between the anode and cathode. To minimize internal ohmic losses, the membrane must possess a high proton conductivity, and is commonly formed from Nafion or other perfluorosulfonic acid polymers. When fully hydrated, these polymers exhibit proton conductivites on the order of $1 \times 10^{-1}$ to $1 \times 10^{-2}$ S/cm. For hydrogen PEMFC without active humidification, proton conductivity decreases rapidly with increasing temperaure. For DMFC, membrane swelling allows methanol diffusion directly from anode to cathode decreasing cell efficiency.

To combat dehydration and methanol crossover, the addition of amorphous,[1−4] mesostructured,[5−9] and microporous silicas[10,11] to the perfluorosulfonic acid polymer has been suggested. Silica-based micro- and mesoporous materials possess desirable traits including large internal surface areas, mechanically stable frameworks, chemical inertness, and negligible electronic conductivity. Furthermore, materials functionalized with organic sulfonic acids (through co-condensation or grafting) have shown proton conductivities on the order of Nafion.[7,8,12−16] While a few reports address the use of sulfonic acid functionalized mesoporous materials and zeolites,[11,17] and a nonporous organic carboxylic acid-containing silicate[18] for fuel cell applications, no reports are found on phosphonic and carboxylic acid containg zeolites or mesoporous materials for use in fuel cell membranes. Futher, there is little information on how the pore structure (i.e., pore size and dimensinality) may influence proton transport under conditions of similar acid loading. Here, zeolite beta, MCM-41, and MCM-48 samples are compared to address the effects of acid strength, pore size, and dimensionality on proton conductivity.

Organically functionalized zeolite beta (denoted BEA), MCM-41, and MCM-48 containing phenyl sulfonic acid, propyl sulfonic acid, ethyl phosphonic acid, or ethyl carboxylic acid were prepared to test the effects of pore structure and acid strength on proton conductivity. Four organic silanes are incorporated into pure-silica zeolite beta by direct synthesis and grafted onto the surfaces of calcined MCM-41 and MCM-48. The attached organic moieties are then converted into acid functional groups and the resulting solid acids are investigated for their ability to transport protons. Detailed synthesis procedures are provided in the Supporting Information.

Powder X-ray diffraction verifies crystalline products with the *BEA framework topology, MCM-41 pore structure and MCM-48 pore structure (see the Supporting Information, Figure S2). $^{29}$Si CPMAS NMR data confirm the silicon−carbon connectivity between the organic groups and inorganic structure (see the Supporting Information, Figure S3). T3 peaks are visible in BEA samples, whereas T3, T2, and T1 resonances are observed in the grafted MCM-41 and MCM-48 materials indicating successful attachment of organic silanes. $^{13}$C CPMAS NMR spectra (see the Supporting Information, Figure S4) were used to verify the presence of the incorporated organic group, with the exception of the

* Corresponding author. E-mail: mdavis@cheme.caltech.edu.
[†] California Institute of Technology.
[‡] University of California, Riverside.

(1) Watanabe, M.; Uchida, H.; Seki, Y.; Emori, M.; Stonehart, P. *J. Electrochem. Soc.* **1996**, *143* (12), 3847–3852.
(2) Adjemian, K. T.; Lee, D. J.; Srinivasan, S.; Benziger, J.; Bocarsly, A. B. *J. Electrochem. Soc.* **2002**, *149* (3), A256−A261.
(3) Ladewig, B. P.; Knott, R. B.; Hill, A. J.; Riches, J. D.; White, J. W.; Martin, D. J.; Costa, J. C. D. d.; Lu, G. Q. *Chem. Mater.* **2007**, *19*, 2372–2381.
(4) Mauritz, K. A. *Mater. Sci. Eng., C* **1998**, *6*, 121–133.
(5) Baglio, V.; Di Blasi, A.; Arico, A. S.; Antonucci, V.; Antonucci, P. L.; Trakanprapai, C.; Esposito, V.; Licoccia, S.; Traversa, E. *J. Electrochem. Soc.* **2005**, *152* (7), A1373−A1377.
(6) Kim, H. J.; Lim, J. E.; Shul, Y. G.; Han, H. Mesoporous silica: Polymer composite membrane for direct methanol fuel cell. In *Recent Advances in the Science and Technology of Zeolites and Related Materials, Pts. A−C*, Proceedings of the 14th International Zeolite Conference, Cape Town, South Africa, April 24−30, 2004; Elsevier: Amsterdam, 2004;Vol. 154, pp 3036−3043.
(7) Hogarth, W. H. J.; da Costa, J. C. D.; Drennan, J.; Lu, G. Q. *J. Mater.Chem.* **2005**, *15* (7), 754–758.
(8) Lin, Y.-F.; Yen, C.-Y.; Ma, C.-C. M.; Liao, S.-H.; Lee, C.-H.; Hsiao, Y.-H.; Lin, H.-P. *J. Power Sources* **2007**, *171*, 388–395.
(9) Pereira, F.; Valle, K.; Belleville, P.; Morin, A.; Lambert, S.; Sanchez, C. *Chem. Mater.* **2008**, *20* (5), 1710–1718.
(10) Li, X.; Roberts, E. P. L.; Holmes, S. M.; Zholobenko, V. *Solid State Ionics* **2007**, *178*, 1248–1255.
(11) Chen, Z. W.; Holmberg, B.; Li, W. Z.; Wang, X.; Deng, W. Q.; Munoz, R.; Yan, Y. S. *Chem. Mater.* **2006**, *18* (24), 5669–5675.
(12) Halla, J. D.; Mamak, M.; Williams, D. E.; Ozin, G. A. *Adv. Funct. Mater.* **2003**, *13* (2), 133–138.
(13) Marschall, R.; Bannat, I.; Caro, J.; Wark, M. *Microporous Mesoporous Mater.* **2007**, *99*, 190–196.
(14) Otomo, J.; Wang, S.; Takahashi, H.; Nagamoto, H. *J. Membr. Sci.* **2006**, *279*, 256–265.
(15) Li, H.; Nogami, M. *Adv. Mater.* **2002**, *14* (12), 912–914.
(16) Mikhailenko, S.; Desplantier-Goscard, D.; Danumah, C.; Kaliaguine, S. *Microporous Mesoporous Mater.* **2002**, *52*, 29–37.
(17) Holmberg, B. A.; Hwang, S.-J.; Davis, M. E.; Yan, Y. *Microporous Mesoporous Mater.* **2005**, *80*, 347–356.
(18) Alabi, C. A.; Davis, M. E. *Chem. Mater.* **2006**, *18* (24), 5634–5636.

10.1021/cm801418r CCC: $40.75 © 2008 American Chemical Society
Published on Web 08/06/2008

**Table 1. Summary of Proton Conductivity and Acid Loading[a]**

| sample identity | $\sigma$ (S/cm) | TGA loading (mmol/g) | acid loading (mequiv/g) |
|---|---|---|---|
| BEA | $8.8 \times 10^{-6}$ | | −0.003 |
| MCM-41 | $2.9 \times 10^{-5}$ | | 0.0055 |
| MCM-48 | $3.5 \times 10^{-5}$ | | 0.0053 |
| O-BEA | $1.5 \times 10^{-5}$ | | 0.0012 |
| O-MCM-41 | $2.3 \times 10^{-5}$ | | 0.0052 |
| PE-BEA | $2.9 \times 10^{-5}$ | 0.22 | 0.0099 |
| PE-MCM-41 | $1.6 \times 10^{-5}$ | 0.27 | 0.09 |
| C-BEA | $1.1 \times 10^{-5}$ | 0.06 | 0.1 |
| P-BEA | $1.0 \times 10^{-4}$ | 0.04 | 0.21 |
| S-MP-BEA | $4.4 \times 10^{-4}$ | [b] | 0.15 |
| S-PE-BEA | $5.4 \times 10^{-4}$ | 0.17 | 0.18 |
| S-PE-BEA-100[c] | $6.7 \times 10^{-3}$ | 0.24 | 0.30 |
| S-PE-BEA-50[c] | $4.9 \times 10^{-3}$ | 0.19 | 0.23 |
| C-MCM-41 | $2.4 \times 10^{-5}$ | 0.43 | 0.35 |
| P-MCM-41 | $3.2 \times 10^{-4}$ | 0.20 | 0.41 |
| S-MP-MCM-41 | $6.9 \times 10^{-4}$ | 0.33 | 0.31 |
| S-PE-MCM-41 | $2.4 \times 10^{-3}$ | 0.34 | 0.34 |
| C-MCM-48 | $2.5 \times 10^{-5}$ | 0.36 | 0.30 |
| P-MCM-48 | $1.1 \times 10^{-3}$ | 0.19 | 0.36 |
| S-MP-MCM-48 | $2.7 \times 10^{-3}$ | 0.29 | 0.23 |
| S-PE-MCM-48 | $3.9 \times 10^{-3}$ | 0.29 | 0.28 |

[a] O, Oleum treated; S, sulfonated; PE, phenethyl; MP, mercaptopropyl; P, phosphonic acid containing, C, carboxylic acid containing. [b] Could not determine from TGA due to overlap with residual $TEA^+$, [c] data from ref 22.

phosphonic acid containg materials. $^{31}P$ CPMAS NMR spectra for the phosphoric acid containg materials are shown in the Supporting Information, Figure S5. Thermogravimetric analysis (TGA) is used to estimate the organic loading in each material, and representative TGA traces are shown in the Supporting Information, Figure S6. TGA loadings are corroborated by acid titration (samples contacted with excess 0.01 N NaOH followed by back-titration with 0.01 N HCl). Fourier transform-infrared spectroscopy (FTIR) further verifies postgrafting chemical modification to produce phosphonic and carboxylic acids (see the Supporting Information, Figure S7).

To assess the ability of the acid-functionalized materials to act as solid electrolytes, impedance spectroscopy is employed. A Solartron 1260 is used to measure the frequency response of samples, equilibrated with bulk water at room temperature, from 1 Hz to 5 MHz with a 100 mV applied signal.[16−19] A schematic of the experimental setup is shown in the Supporting Information, Figure S1. The proton conductivity is calculated from the low frequency real-axis intercept of the commonly observed semicircular arc by scaling the resistance appropriately with pellet thickness and pellet diameter. Only one semicircular arc is observed over the scanned frequency range. Representative impedance data are shown in the Supporting Information, Figure S8.

Proton conductivity results, organic loadings approximated from thermogravimetric analysis, and acid loadings determined from titration are presented in Table 1 for comparison. Although care was taken to prepare samples with as similar acid loadings as possible, there is slight variation in the measured acid loadings between samples. These differences, however, are not believed to greatly affect the conclusions, and Table S1 in the Supporting Information shows data for MCM-41 samples with higher organic acid loading, but exhibiting the same trends as those discussed below.

Unfunctionalized, pure-silica materials (MCM-41, MCM-48, BEA) exhibit proton conductivities on the order of $1 \times 10^{-5}$ S/cm and treatement with fuming sulfuric acid (O-BEA, O-MCM-41) does not significantly affect these values. MCM-41 and MCM-48 both exhibit slightly higher conductivity than BEA, most likely because of an increased number of surface hydroxyl groups. Measurements were also made on phenethyl-functionalized materials prior to sulfonation with oleum, and these nonacidic, organic-containing samples (PE-BEA, PE-MCM-41) exhibit proton conductivities similar to nonfunctionalized materials.

When samples have acidic organic groups, trends in the proton conductivities within each family of materials exist. Aryl sulfonic acid materials exhibit the highest conductivity values followed by propyl sulfonic acid containing samples, then phosphonic acid functionalized materials, and finally carboxylic acid functionalized materials. This trend of decreasing proton conductivity correlates well with acid strength of organic acid in solution. Acid-functionalized materials exhibit higher conductivity than the unfunctionalized parent materials with the exception of the carboxylic acid containing samples, which show nearly the same conductivity as the unfunctionalized materials. This is not surprising as the $pK_a$ of propylcarboxylic acid (4.88) is in the range of suggested $pK_a$ values for surface hydroxyls of hydrated silica under aqueous conditions.[20−22]

Acid-functionalized BEA materials (S-PE-BEA, S-MP-BEA, P-BEA, C-BEA) exhibit the lowest proton conductivities for each functionality when compared to MCM-41 and MCM-48 with the same organic functionality. As is shown in a recent report,[23] this is due to the hydrophobic nature of the nearly hydroxyl-defect-free framework, leading to a less complete hydrogen bonding water network for Grotthüss transport.

Interestingly, acid-functionalized MCM-48 samples exhibit higher proton conductivity than the corresponding MCM-41 sample. This observation may arise because of the three-dimensional interconnected pore structure of MCM-48 as compared to the one-dimensional pore structure of MCM-41. MCM-41 particles may have their one-dimentional pores aligned perpendicular to the applied electric field, appearing electrically as series resistance, leading to lower measured conductivity as there is no driving force for proton motion along the direction of the pore.

A further comparison can be made between S-PE-MCM-48 and S-PE-BEA-100. S-PE-BEA-100 is an organically functionalized zeolite beta sample (see ref 22 for synthesis details) crystallized from an aluminum containing gel ($SiO_2$/

(19) Mikhailenko, S. D.; Kaliaguine, S.; Ghali, E. *Microporous Materials* **1997**, *11*, 37–44.

(20) Iler, R. K., *The Chemistry of Silica: Solubility, Polymerization, Colloid and Surface Properties, and Biochemistry*; John Wiley & Sons: New York, 1979.

(21) Rosenholm, J. M.; Czuryszkiewicz, T.; Kleitz, F.; Rosenholm, J. B.; Linden, M. *Langmuir* **2007**, *23*, 4315–4323.

(22) Ong, S.; Zhao, X.; Eisenthal, K. B. *Chem. Phys. Lett.* **1992**, *191* (3−4), 327–335.

(23) McKeen, J. C.; Yan, Y. S.; Davis, M. E. *Chem. Mater.* **2008**, *20*, 3791–3793.

$Al_2O_3 = 100$) using tetraethylammonium hydroxide (instead of the tetraethylammonium fluoride used in the synthesis of the pure silica BEA samples), and has hydroxyl groups like MCM-48. Both S-PE-MCM-48 and S-PE-BEA-100 have interconnected three-dimensional pore structures and exhibit nearly identical acid loadings by TGA and titration. While the measured conductivities of both of these samples are within the same order of magnitude, the microporous zeolite beta appears to transport protons at a slightly faster rate than the mesoporous MCM-48 sample.

S-PE-BEA-50, also synthesized from an aluminum containing gel ($SiO_2/Al_2O_3 = 50$) using tetraethylammonium hydroxide, shows a slightly lower loading than both S-PE-BEA-100 and S-PE-MCM-48 by titration and TGA but has an intermediate proton conductivity, $\sim 5 \times 10^{-3}$ S/cm. The loading, however, is nearly the same as S-PE-BEA, the pure-silica sample with very little hydroxyl groups. The conductivity of S-PE-BEA, however, is an order of magnitude less than S-PE-BEA-50. As discussed in our recent report,[23] this is attributed to the higher number of hydroxyl groups in zeolite beta samples crystallized from hydroxide containing synthesis gels.

From a device perspective, where proton conductivity is to be maximized to reduce internal ohmic losses, hydroxyl groups are clearly necessary, but further considerations exist. Meanwhile, S-PE-MCM-48 and S-PE-BEA-100(50) exhibit similar proton conductivity ($\sim 5 \times 10^{-3}$ S/cm), the small pores of zeolite beta may better inhibit the crossover of methanol from the anode to the cathode, eliminating one cause of decreased efficiency. The small zeolitic pores may also retain water at high temperatures better than the mesopores of MCM-41 or MCM-48. Admittedly, particle size, which does not seem to affect the measured conductivy,[17,23] may play a role in the reduction of methanol crossover if these powder materials are successfully fabricated into membranes, but methanol crossover measurements are beyond the scope of this investigation.

In conclusion, pure-silica zeolite beta, MCM-41, and MCM-48 containing sulfonic acids, phosphonic acid, or carboxylic acid were prepared and investigated for use as solid electrolytes. Aryl sulfonic acid containing samples exhibit the highest measured proton conductivity values, follwed by propyl sulfonic acid containing materials, phosphoric acid containg materials and carboxylic acid materials that were approximately the same as nonorganically modified silicas. MCM-41 and MCM-48 show higher proton conductivities than corresponding pure-silica zeolite beta samples, and MCM-48 samples are more conductive than corresponding MCM-41 samples. An aryl sulfonic acid functionalized zeolite beta sample with hydroxyl groups, however, appears to be a slightly better proton conductor than the corresponding MCM-48 sample functionalized to the same acid loading level.

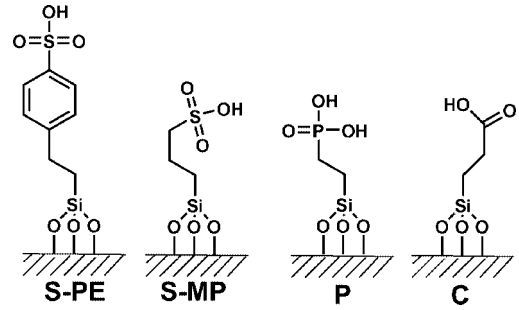


**Figure 1.** Illustration of the acid groups incorporated into zeolite beta, MCM-41, and MCM-48.

**Acknowledgment.** We acknowledge the U.S. Department of Energy (DE-FG02-05ER15716) and US National Science Foundation (CTS-0404376) for funding. J.C.M. acknowledges the John and Fannie Hertz Foundation and the NSF National Science Foundation Graduate Research Fellowship Program for financial support.

**Supporting Information Available:** X-ray, NMR, TGA, FTIR, impedance spectra, and experimental details (PDF). This material is available free of charge via the Internet at http: //pubs.acs.org.

CM801418R